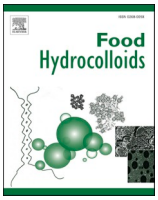
Food Hydrocolloids 157 (2024) 110427



Contents lists available at ScienceDirect

Food Hydrocolloids

journal homepage: www.elsevier.com/locate/foodhyd





Bacterial cellulose nanocrystals or nanofibrils as Pickering stabilizers in low-oil emulsions: A comparative study

Náyra O.F. Pinto [a,d,**], Ana Isabel Bourbon [b], Daniela Martins [c], André Pereira [a], Miguel A. Cerqueira [b], Lorenzo Pastrana [b], Miguel Gama [c], Henriette M.C. Azeredo [e], Morsyleide F. Rosa [a,d,***], Catarina Gonçalves [b,*]

[a] Embrapa Tropical Agroindustry, Rua Dra. Sara Mesquita, 2270, 60511-110, Fortaleza, CE, Brazil
[b] International Iberian Nanotechnology Laboratory, Avenida Mestre José Veiga, 4715-330, Braga, Portugal
[c] Centre of Biological Engineering, University of Minho, Braga, Portugal
[d] Department of Chemical Engineering, Federal University of Ceará, Fortaleza, CE, Brazil
[e] Embrapa Instrumentation, Rua XV de Novembro, 1452, 13560-970, São Carlos, SP, Brazil

ARTICLE INFO

Keywords:
Bacterial cellulose
Oil-in-water food emulsion
Nanocrystals
Nanofibrils
Pickering emulsions
Low-oil emulsions

ABSTRACT

This investigation assessed the potential of bacterial cellulose (BC) in two distinct forms, nanocrystals (BC-NC) and oxidized nanofibrils (BC-NF), as stabilizers for low oil-in-water emulsions (1 % v/v). The research explored the impact of ionic strength and BC concentration on the physico-chemical characteristics, stability, and rheological properties of those emulsions. Nanofibrils had diameters ranging from 25 to 146 nm and lengths in the micrometer range, while nanocrystals varied in length from 133 to 870 nm and in diameter from 20 to 60 nm. Both BC-NF and BC-NC exhibited high zeta potential values (>−45 mV) and contact angles of 30-31°, indicating stability. Both nanocelluloses were effectively used as stabilizers in Pickering emulsions, namely in low-oil systems, producing small emulsion droplets with sizes between 1.42 and 4.13 μm. Further results revealed that ionic strength influenced emulsion stability, with both BC-NF and BC-NC preferentially located on the surfaces of emulsion droplets in the presence of salt, as demonstrated by microscopy images. The presence of BC at the interface contributed to creating a more robust barrier against coalescence and Ostwald ripening, influencing droplet size and rheological properties. Higher BC concentrations (1 %) increased emulsion stability in the absence of salt, while at lower BC concentrations (0.5 %), salt concentration was determinant for the long-term stability of the emulsions. These findings provide valuable insights into the production of Pickering emulsions using nanocelluloses, highlighting the advantages of bio-based nanomaterials for applications in the food industry.

1. Introduction

In the food industry, oil-in-water emulsions are usually stabilized by food-grade emulsifiers, such as proteins, phospholipids, surfactants, and polysaccharides. These emulsifiers are adsorbed at the oil-water interface, protecting emulsion droplets from aggregation, mainly through the reduction of interfacial tension (Cai et al., 2023).

The most used emulsifiers in the food industry are small-molecule surfactants, amphiphilic biopolymers, and surface-active particulate matter (Jiang et al., 2020). Although conventional emulsifiers (i.e., surfactants) have been successfully used, their consumption has received research attention in recent years due to preliminary evidence of adverse effects on human health (Chassaing et al., 2015; Cox et al., 2021; Jia et al., 2016; Jiang et al., 2020; Naimi et al., 2021; Rhodes, 2021; Viennois et al., 2020). Consequently, emulsion science has driven the development of new approaches to improve food quality and functionality (Bai et al., 2021).

In this framework, emulsions armored by a layer of solid particles at

* Corresponding author. Food Processing and Nutrition Research Group, International Iberian Nanotechnology Laboratory, Av. Mestre José Veiga s/n, Braga, Portugal, 4715-330.
** Corresponding author. Embrapa Tropical Agroindustry, Rua Dra. Sara Mesquita, 2270, 60511-110, Fortaleza, CE, Brazil.
*** Corresponding author. Department of Chemical Engineering, Federal University of Ceará, Fortaleza, CE, Brazil.
E-mail addresses: nnayrapinto@alu.ufc.br (N.O.F. Pinto), morsyleide.rosa@embrapa.br (M.F. Rosa), catarina.goncalves@inl.int (C. Gonçalves).

https://doi.org/10.1016/j.foodhyd.2024.110427
Received 13 March 2024; Received in revised form 8 July 2024; Accepted 15 July 2024
Available online 16 July 2024
0268-005X/© 2024 The Authors. Published by Elsevier Ltd. This is an open access article under the CC BY license (http://creativecommons.org/licenses/by/4.0/).

the oil-water interface have been developed, known as Pickering emulsions that are surfactant-free and highly stable (Bai et al., 2021). Pickering emulsions typically have strong resistance to coalescence due to the almost irreversible attachment of colloidal particles to the droplet's surface, replacing the surfactants (Ming et al., 2023; Morais et al., 2023). Different solid particles, presenting affinity for both phases (amphiphilicity) that result in appropriate wetting properties, have been used as stabilizers in Pickering emulsions, including both inorganic and organic nanoparticles (Fujisawa et al., 2017). Bio-based nanomaterials, such as polysaccharides, fit the clean label movement, a demand that reflects consumers' concern to use more natural food products (Bai et al., 2018; Maruyama et al., 2021. Bacterial cellulose is a biopolymer and, although chemically identical to vegetable cellulose, it is naturally obtained free of lignin and hemicelluloses. Although not regulated in Europe and the USA, bacterial cellulose is used in the food industry in Asia and as an implantable material in various medical applications, demonstrating its safety. However, this applies to bacterial cellulose, not yet to nano-derivatives (Mota et al., 2022). Reducing the size of its fibrillar structure through physical and/or chemical processes generates structures in the form of nanofibrils (BC-NF) or nanocrystals (BC-NC). These nanocelluloses exhibit unique properties resulting from their structure and surface chemistry with great potential to stabilize food emulsions (Azeredo et al., 2019; Koshani & Madadlou, 2018; Liu et al., 2022; Mikulcová et al., 2023; Wong et al., 2023)

The ability of cellulose-based nanostructures to assemble at oil-water interfaces is particularly useful and has led to recent articles and patents in this area (Kedzior et al., 2021). Factors affecting the capacity to stabilize oil-in-water emulsions include the source, shape, particle size, surface charge density, and concentration of nanocellulose (Low et al., 2020). Studies with nanocellulose have been limited to the use of oil fractions higher than 10 %, with emphasis on emulsions with high internal phase (HIPEs, an internal phase volume fraction >74 %) (Bago Rodriguez & Binks, 2022; Huang et al., 2024; Kalashnikova et al., 2011; Z. Liu et al., 2021; Paximada et al., 2016; Sommer & Staroszczyk, 2023; Wang et al., 2023; Wu et al., 2023; Yan et al., 2017; K. Zhang et al., 2024; S. Zhang et al., 2023) which can be seen as a high concentration when considering applications targeting multiphase systems, such as beverages and soft drinks (Bai et al., 2018), low-fat foods (Gao et al., 2023; Zhao et al., 2023) or when aiming to minimize the production costs while maintaining the properties and functions of emulsions (Guo et al., 2022). Few studies report Pickering emulsions using nanocellulose with low-oil fractions (<10 %), as well as their application in the food industry. Guo et al. studied the stabilization of 1% oil emulsions using cellulose nanofibrils or TEMPO-oxidized cellulose nanofibrils from plants, as well as the sequential addition of both (Guo et al., 2022). In a different study, synergies of combining plant-based cellulose nanofibrils and nanocrystals, were exploited to stabilize 1% oil emulsions (Bai et al., 2018). The potential applications of low-oil emulsions in the food industry include low-fat dressings and sauces (Ford Kraft Foods et al., 2004).

Indeed, emulsions with low-oil content (Hedayati et al., 2020) or nanoemulsions (McClements, 2012) represent a challenge as they tend to decompose quickly and undergo phase separation due to the reduced amount of dispersed phase. Efficient emulsifiers and processing methods are required to ensure adequate emulsion stability. Emulsions with high volume fraction of the oil phase have their stability improved due to the increase in the packing fraction of oil droplets (Dickinson & Golding, 1997).

Ionic strength has demonstrated a significant impact on the characteristics and stability of Pickering emulsions (Courtenay et al., 2021; Yan et al., 2017), as it imparts surface activity to particles, rendering them effective emulsifiers or facilitating their detachment from the interface as needed (Anjali & Basavaraj, 2018). However, no attempts have been reported for the production of low-oil, oil-in-water, Pickering emulsions stabilized through charge modulation by ionic strength. The individual effect of nanocrystals or nanofibrils on the formation and stability of such emulsions has not been explored, so far. In summary, finding effective approaches to produce stable Pickering emulsions using bacterial nanocelluloses in emulsion systems with low-oil concentration is particularly relevant for the synthesis of food (McClements, 2015), cosmetics (Chuberre et al., 2019; Mohiuddin, 2019), and other green materials (Moustafa et al., 2022).

In this study, the use of bacterial nanocelluloses (BC-NF or BC-NC) as stabilizers in the production of Pickering emulsions with low-oil concentration (1 % v/v) was proposed. The effects of ionic strength (up to 50 mM NaCl) and nanocellulose concentration (up to 1 % w/w) on physico-chemical, stability, and rheological properties were evaluated. According to the EU policy, a low salt claim can be done for products using NaCl concentrations lower than 51 mM. The NaCl concentrations tested in this work are within the low salt range of the EU policy. Nanocrystals and nanofibrils were produced using different methodologies, resulting in variations in shape, size, and surface charge. To the best of our knowledge, this is the first work comparing BC-NF and BC-NC as natural emulsifiers on the development of Pickering emulsions with a low-oil fraction (1 %). This research showed the formation of individualized nanocrystals or nanofibrils networks as effective stabilizers in low-oil fraction emulsion systems, which can be manipulated by controlling the concentration of salt or bacterial nanocellulose.

2. Materials and methods

2.1. Materials

Purified bacterial cellulose (BC) membranes produced by *Komagataeibacter xylinus* ATCC 53582, by fermentation under static conditions in a synthetic HS medium (do Nascimento et al., 2019), were provided by Embrapa Tropical Agroindustry (Brazil). Potassium bromide (NaBr), sodium hypochlorite (NaClO), sodium hydroxide (NaOH), and sulfuric acid (H_2SO_4) were obtained from VETEC (Rio de Janeiro, Brazil) and used without further purification and as received from the supplier. Dialysis bag, 2,2,6,6-tetramethyl-1-piperidinoxyl (TEMPO), formvar, and phosphotungstic acid were purchased from Sigma-Aldrich Co (São Paulo, Brazil).

Sodium chloride (NaCl) was purchased from Sigma-Aldrich Co. (Helsinki, Finland). Commercial refined sunflower oil (3ás, Fula, Sovena Group, Algés, Portugal) was purchased from a local supermarket (Braga, Portugal) and isohexadecane was gently provided by Lanxess (Leverkusen, Germany). β-carotene (Type II, synthetic, ≥95 % (HPLC), crystalline) was purchased from Sigma Aldrich (Saint Louis, MO, USA). Ultrapure water was used throughout the experiments (Milli-Q, Darmstadt, Germany).

2.2. Preparation of oxidized BC nanofibrils (BC-NF)

BC was oxidized through TEMPO-mediated oxidation and nanofibrillated following the method proposed by Pereira et al. (Pereira et al., 2020). BC was suspended in distilled water (10 mg/mL, dry basis) containing dissolved TEMPO and NaBr (0.016 g and 0.1 g per gram of BC, respectively). Oxidation was initiated by adding an 11 % NaClO solution (sufficient to achieve a NaClO concentration of 5 mmol/g based on dry BC) to the suspension at 25 °C under stirring (500 rpm). The pH was adjusted to 10–10.5 with a 0.5 mol L^{-1} NaOH solution, and the conditions were maintained for 150 min. Ethanol (95 % v/v) (60 mL per gram of BC) was added to halt the reaction. The oxidized BC was washed with water and centrifuged at 26,400×*g* for 15 min (Hitachi - CR 22GIII) until reaching pH ~ 6.5. The BC-NF suspension was prepared by disintegrating the oxidized BC using a high-speed mixer (Vita-Prep 3, Vitamix Corp., Cleveland, OH, USA) at 24,000 rpm for 15 min. The solid content of the suspension was determined gravimetrically after drying at 105 °C to a constant weight, and the carboxylate content of BC-NF was determined by the electrical conductivity titration method (Digimed, model DM-32, São Paulo, Brazil).

2.3. Preparation of bacterial cellulose nanocrystals (BC-NC)

Bacterial cellulose nanocrystals (BC-NC) were prepared through acid hydrolysis conducted at 45 °C for 90 min using 60 % (w/w) sulfuric acid. Bacterial cellulose pulp (10 g) was stirred in 200 mL of the acid solution. At the end of the process, the reaction was halted by adding cold deionized water (~4 °C) in a volumetric ratio of 1:3 (suspension/water, v/v). The suspension was centrifuged (Hitachi - CR 22GIII) at 26,400×*g* for 15 min at 20 °C until the supernatant became clear. The resulting BC-NCs were washed in three cycles with deionized water and centrifuged at 26,400×*g* for 15 min at 20 °C. Ultrasonication (Unique – Cell Disruptor, 60 Hz; 300W) was applied in each cycle for 2 min, interspersed with 1 min intervals to prevent particle agglomeration. Subsequently, the colloidal suspension was dialyzed with distilled water for 48 h until reaching a pH of ~ 6.5. The BC-NC suspension was a mixture of three batch suspensions, and its solid content was determined gravimetrically after drying at 105 °C to a constant weight.

2.4. Physico-chemical characterization of bacterial nanocelluloses

2.4.1. Zeta potential measurements

The zeta potential of aqueous nanocellulose diluted 100 × in Milli-Q water was measured using dynamic light scattering (DLS) with a Zetasizer Nano ZS (Malvern Instruments Ltd., Worcestershire, UK Kingdom) at 25 °C, using a detection angle adjustment of 173°, refractive index 1.45, dispersion index 1.33, viscosity 0.8872 cP and He–Ne laser (4 nW). The electrophoretic mobility considered the water dielectric constant of 78.5. The Zetasizer Software (version 7.03) was applied to analyze the data.

2.4.2. Transmission electron microscopy (TEM)

Morphological analysis was performed using a microscope Tescan Vega 3 SBU (Tesca, Czech Republic), with a STEM detector under an acceleration voltage of 30 kV. 100 × diluted suspensions of BC-NF or BC-NC were deposited onto individual grids covered with Formvar, and the excess suspension was removed with absorbent paper. After 3 min, drops of 1 % (w/v) phosphotungstic acid were deposited on the grids and removed with absorbent paper. At least 10 fields from the sample holder were viewed. The average diameters or lengths of the nanofibrils and nanocrystals of at least 100 structures were determined using the ImageJ software (National Institute of Health-NIH, America) (Vasconcelos et al., 2017).

2.4.3. Fourier-transform infrared spectroscopy (FTIR)

FTIR spectra of BC-NC and BC-NF were recorded in absorption mode using a VERTEX 80v FTIR spectrometer (Bruker, Germany) in the wavelength range 4000-400 cm^{-1} at a resolution of 4 cm^{-1} over 32 scans, using the Platinum Attenuated Total Reflection mode (ATR) (Bruker, Germany). FTIR spectra were normalized between 0 and 1. Samples were frozen (−80 °C) and then freeze-dried (−50 °C) under 1.09 Pa for 48 h and stored until further characterization.

2.4.4. Contact angle and interfacial tension

The contact angle and interfacial tension of the BC-NF or BC-NC suspensions were determined by a dynamic contact angle measuring device (OCA 20, DataPhysics) and SCA 20 Software module 20 (DataPhysics).

To measure the contact angle, three overlapping layers (~100 μL each) of BC-NF or BC-NC suspensions (1 %) were dried at 37 °C on glass slides to obtain flat and uniform films. Using a 500 μL Hamilton syringe, 2 μL of double distilled water droplet was deposited in the film's surfaces using a high-precision injector. The contact of water with the films was recorded with a contact time of 120 s at 20 ± 1 °C. Ten measurements were taken for each material.

The interfacial tension as a function of BC-NF dosage (0.5 %, 1 %) or BC-NC dosage (0.5 %, 1 %) was measured by the pendant drop method (Martins et al., 2020). Sunflower oil or isohexadecane (2 mL) was added to a disposable optical polystyrene macro standard fluorescent cuvette (1 cm × 1 cm × 4.5 cm) (Labbox). A pendant drop of the suspensions was formed using a disposable 1 mL syringe with a needle of 0.71 mm outer diameter immersed in the oily phase, always at the same depth. The maximum volume of the drops was determined for each sample beforehand. The interfacial tension value was automatically calculated, 10 times per minute up to 25 readings, in triplicate for each sample and at 20 ± 1 °C.

2.5. Preparation of oil-in-water Pickering emulsions

Emulsions with low sunflower oil fraction (1 % v/v) were prepared by mixing BC-NF or BC-NC (0.5–1 % v/v) with or without NaCl (up to 50 mM) in triplicate. After combining the components, the mixture was immediately emulsified using a high shear force mixer (IKA Ultra - Turrax T-18 digital) at 20,000 rpm for 4 min and then sonicated (Sonifier 450, Branson Ultrasonics, Danbury, CT) in an ice bath for 4 min, with 30 s on/off time and 50 % amplitude for every emulsion. This corresponds to a power density of approximately 20,000 $W.L^{-1}$ of emulsion. All emulsions were analyzed to determine the average droplet size and morphology. Emulsion stability was also evaluated by visual inspection, considering that the absence of oil or creaming on the emulsion surface means emulsion stability.

2.6. Physico-chemical characterization of Pickering emulsions

2.6.1. Droplet size - optical microscopy

Images of the emulsions were captured with an optical microscope Wide-Field Upright Fluorescence Microscope – Nikon – Ni-E equipped with a Nikon DS-Fi2 camera (Nikon, Japan) within 180 min after emulsion preparation. A droplet of the emulsion was pipetted onto a glass slide and gently spread on the slide using the tip. The use of cover glasses was avoided and only applied when necessary for acquiring images. Samples were studied at 5 × , 20 × , and 50 × magnifications. The particle size of the emulsions was measured from images with 50 × magnification and analyzed using the ImageJ software (National Institute of Health-NIH, America). According to Mie's theory, particle size measurements were reported as the weighted average diameter per area $D_{(3,2)}$ and calculated as follows (Eq. (1)) (Wu et al., 2022).

$$D_{(3.2)} = \frac{\sum n_i \times d_i^3}{\sum n_i \times d_i^2} \quad (1)$$

where, n_i is the number of the particles with the diameter d_i.

2.6.2. Stability

2.6.2.1. Stability at room temperature. The effect of BC-NF or BC-NC concentration (0.5–1 wt %) and ionic strength (0, 12.5, and 50 mM NaCl) was evaluated on the stability of freshly prepared or after 30 days of storage emulsions. Emulsions were stored in test tubes at room temperature and sealed with aluminum foil to prevent water evaporation. Stability was assessed through visual inspection of the emulsion and optical microscopy.

2.6.2.2. Accelerated stability. Accelerated stability towards centrifugal forces was also evaluated by submitting emulsions to centrifugation according to Gestranius et al. (Gestranius et al., 2017). 30 min after preparation, emulsions (1 mL) were centrifuged (Centrifuge 5810, Eppendorf, Germany) for 2 min at 1520 *g*. The emulsions were inspected visually (coalescence and forced creaming) and by optical microscopy.

2.6.3. Cryo-SEM

Cryo-SEM observations were performed using a high-resolution scanning electron microscope (JEOL JSM 6301 F) with X-ray

microanalysis (Oxford INCA Energy 350) and Cryo-SEM experimental facilities (Gatan Alto 2500). Each sample was rapidly cooled in liquid nitrogen and transferred, under vacuum, to the cold stage of the preparation chamber. The specimen was fractured, sublimated for 120 s at -90 °C, and coated with Au/Pd by sputtering for 50 s with a 12 mA current. The sample was then transferred into the SEM chamber and observed at a temperature of −150 °C (Martins et al., 2020).

2.6.4. Confocal laser scanning microscopy (CLSM)

To observe the aqueous and oily phases, an oil-in-water emulsion stabilized by BC-NC was prepared using sunflower oil (10 % v/v) incorporating beta-carotene (0.05 % w/v) and stabilized by BC-NC (1 % v/v) containing 50 mM NaCl. Confocal Laser Scanning microscope (Zeiss LSM 780, Germany) was utilized to investigate the effective adsorption of bacterial cellulose particles on the oil-water interface.

Briefly, 100 μL emulsion was incubated with 10 μL of CalcoFluor White (1 mg/mL) (Sigma-Aldrich,USA) for 15 min to stain cellulose. CalcoFluor was observed at an excitation wavelength of 405 nm. The natural fluorescence of beta-carotene in the oil phase was visualized at an excitation wavelength of 488 nm. The optical resolution of the digital images was 512 pixels x 512 pixels. Images were digitally recorded and processed using the equipment's software (Zen 2010 software and image).

2.6.5. Rheology

Flow curves were obtained using a Discovery Hybrid Rheometer (DHR1) from TA Instruments (New Castle, USA) with the Peltier temperature set to 25 °C. TRIOS Software (New Castle, UK) was used to control the equipment and acquire rheological parameters. A stainless-steel cone-plate geometry of 60 mm, with an angle of 2.006° and truncation of 64 μm, was used due to its capability of generating a uniform shear rate across the samples. Steady-state flow curves were obtained working in a controlled-stress mode over the shear rate range of 0.1–100 s. All the samples were measured in triplicate. The Carreau model (Eq. (2)) was fitted to the experimental data (Rao, 2014):

$$\eta_{ap} = \eta_{\infty} + \frac{\eta_0 - \eta_{\infty}}{\left[1 + \left(\frac{\gamma}{\dot{\gamma}c}\right)^{\lambda}\right]^{N}} \quad (2)$$

where η_{ap} is the apparent viscosity (Pa.s), γ is the shear rate (s-1), η_{∞} is the apparent viscosity at the infinite shear rate (Pa.s), η_0 is the apparent viscosity at zero shear rate (Pa.s), N is the dimensionless exponent and $\dot{\gamma}c$ is the critical shear rate (s-1) which marks the end of the Newtonian plateau and/or the beginning of the shear-thinning region.

3. Statistical analysis

Statistical analyzes were performed using Origin Software (version 9.1). The results were expressed as mean ± standard deviation and analyzed statistically by one-way analysis of variance (ANOVA) and Tukey's test at a significance level of $p \leq 0.05$ or *t*-test with a significance level of $p \leq 0.05$.

4. Results and discussion

4.1. Physico-chemical characterization of nanocelluloses: nanofibrils and nanocrystals

Cellulose nanofibrils (BC-NF) were produced through mechanical defibrillation of bacterial cellulose fibers and TEMPO-mediated oxidation. The formation of carboxylic groups on the surface of BC-NF was determined by electric conductivity titration.

Fig. 1a shows the TEM images of BC-NF, where individualized and well-distributed nanofibrils can be observed, with an average diameter of 61 ± 16 nm, ranging from 25 to 146 nm, and a length of several micrometers. The oxidation led to the formation of carboxylate groups (0.77 mmol $COO^{-}.g^{-1}$ cellulose, equivalent to 12.7 %) originating electrostatic repulsions between the cellulose chains, facilitating fibrillation and dispersion in aqueous media while reducing the sample viscosity. The final appearance of the BC-NF dispersion was an opaque and white gel (Fig. 1a).

The sulfuric hydrolysis of bacterial cellulose led to nanocrystals ranging from 133 to 870 nm in length (L) and diameter (d) between 20 and 60 nm, representing an average length ($\bar{L}$) of 425 ± 161 nm and an average width ($\bar{d}$) of 40 ± 7.5 nm, corresponding to an aspect ratio (L/d) of 11. The final appearance of the BC-NC dispersion was a homogeneous turbid dispersion with a solids content of 1.87 % (w/w) (Fig. 1b). Similar appearance was reported for nanocrystals suspension (1 %) obtained from pure vegetable cellulose (Li et al., 2015).

Both nanofibrils and nanocrystals exhibited high (negative) surface

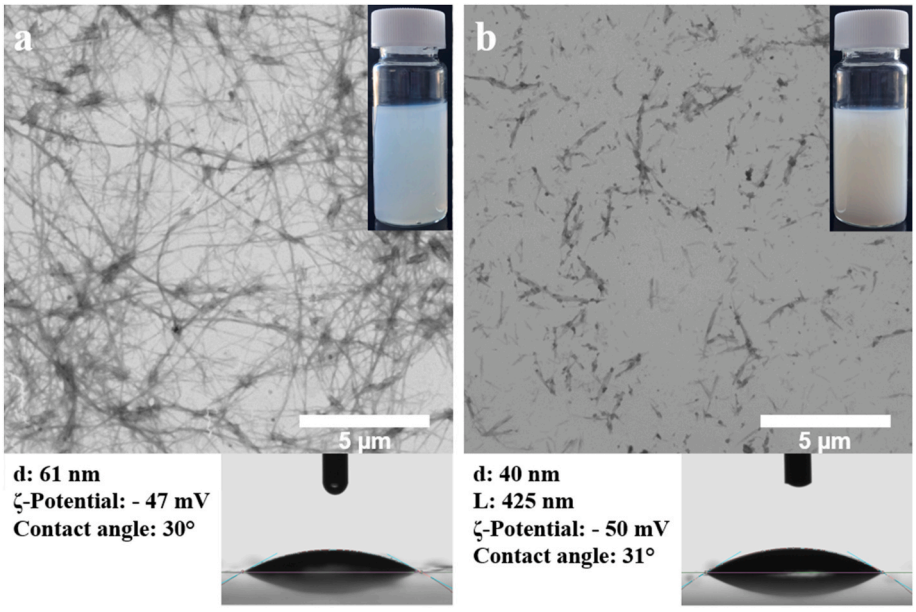


Fig. 1. TEM micrographs, diameter (d), length (L), zeta potential, and contact angle of BC-NF (a) and BC-NC (b). The scale bar is 5 μm. Photographs were taken the day after preparation.

charge in module (>|45| mV), which prevents instability phenomena due to the predominance of electrostatic repulsion forces (Pinto et al., 2016). Stable dispersions of oxidized cellulose nanofibrils, prepared by TEMPO/NaOCl/NaBr oxidation, and nanocrystals, obtained under similar conditions of acid hydrolysis with sulfuric acid, were achieved with zeta potentials of −45.01 ± 5 mV (Courtenay et al., 2021) and −47.96 ± 0.14 mV, respectively (Wu et al., 2021; H. Zhang et al., 2019). Both dispersions (nanocrystals and nanofibrils) remained stable for 12 months when stored in a cold chamber (4 °C).

The wettability of the Pickering material is a key parameter for controlling emulsion stability (Binks & Lumsdon, 2000). This property can be evaluated by measuring the tendency of a liquid to spread over a solid surface, denoted by the contact angle θ (Zeng et al., 2024). Typically, particles with a contact angle <90°, associated with a moderately hydrophilic behavior, tend to stabilize oil-in-water (O/W) emulsions (Bao et al., 2021; Parajuli & Ureña-Benavides, 2022). The contact angle obtained for surfaces containing BC-NF or BC-NC was 30° or 31° (Fig. 1), respectively, indicating high hydrophilicity or wettability, which may not be energetically favorable for particle adsorption at the oil/water interface. Despite the tendency of hydrophilic particles to stay in the aqueous phase, other factors influence the stabilization of a colloidal system. In the presence of salt, for instance, surfaces become neutralized and less hydrophilic, potentially facilitating the migration of particles to the interface, where they can adsorb and contribute to the stabilization of the emulsion. This means that, in practice, Pickering stabilizers with high or low wettability can promote the formation of highly stable oil-in-water emulsions over the long term, considering the emulsification method (Xu et al., 2005), surface charge modulation (Albert et al., 2019), size (Binks & Lumsdon, 2000) or the nature of the particles used (Hu et al., 2020; Kalashnikova et al., 2011; Q. Li et al., 2022).

4.2. Fourier transform infrared spectroscopy (FTIR)

The FTIR spectra of BC-NF or BC-CN are shown in Fig. 2. Vertical lines highlight the characteristic absorption bands of the materials. The spectra showed characteristic bands of cellulose. Both samples showed a broad band at 3340 cm^{-1}, which were attributed to the stretching frequency of the –OH group as well as the intramolecular and intermolecular hydrogen bonds in cellulose (Andrade et al., 2019). The characteristic band around 2892 cm^{-1} was attributed to the H single bond stretching vibration of C-H_2 and C-H_3 groups or asymmetric and symmetric stretching vibrations of CH_2 often found in cellulose fiber components (Khan et al., 2020).

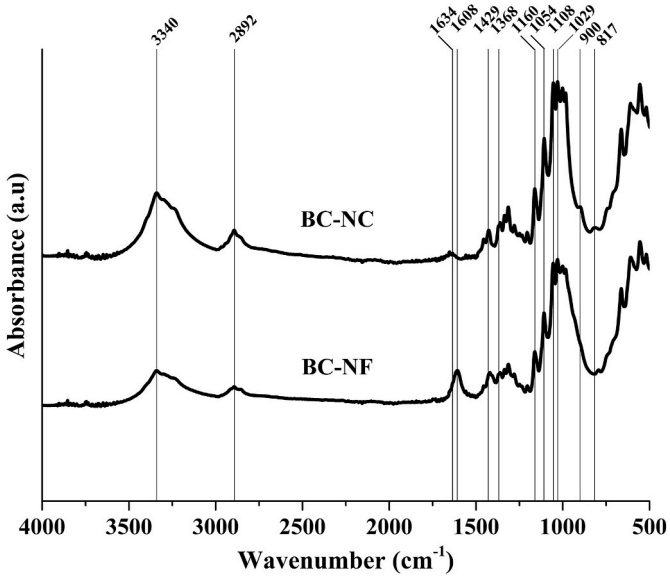


Fig. 2. FTIR spectra of BC-NF and BC-NC suspensions.

The bands at 1429 cm^{-1} and 1368 cm^{-1} were attributed to asymmetric angular deformation of C–H bonds and symmetric angular deformation of C–H bonds, respectively.

Absorption at 1163 cm^{-1} was due to asymmetric stretching of the C-O-C glycosidic bonds and stretching at 1108 cm^{-1} and 1054 cm^{-1} attributed to the C-OH and C-C-OH bonds in secondary and primary alcohols, respectively (Ajkidkarn & Manuspiya, 2020; Vasconcelos et al., 2017). The band around 1029 cm^{-1} corresponds to C-O stretching and a vibration of the amorphous cellulose, resulting from the stretching of the glucose ring, produced a band around 900 cm^{-1} (do Nascimento et al., 2019). The band at 900 cm^{-1} was present with lower intensity in BC-NF due to the strong oxidation reaction that eliminated amorphous cellulose (Pereira et al., 2020). The peak around 817 cm^{-1} was attributed to C-O-C stretching vibration (Pandi et al., 2021).

In the BC-NF spectrum, the 1608 cm^{-1} band, characteristic of the –$COO–Na^+$ group (stretching of the $-COO^-$ group), confirms the presence of carboxylic groups introduced by TEMPO-mediated oxidation (N. Zhang et al., 2016) In the FTIR spectrum of BC-NC, the band at 1634 cm^{-1} was assigned to the absorbed water bending mode (Andrade et al., 2019). In contrast, the band at 807 cm^{-1} (symmetric vibratory bonds of C-O-S bonds of C-O-SO_3- groups) resulting from the esterification of H_2SO_4 in the acid hydrolysis reaction in BC-NC was not detected due to the small amount of sulfate groups attached to vibration (Ajkidkarn & Manuspiya, 2020; Arserim-Uçar et al., 2021; Vasconcelos et al., 2017).

4.3. Interfacial tension at the oil-water interface

The morphological properties (Fujisawa et al., 2017) and concentration (Martins et al., 2020) of nanocellulose have a significant effect on its emulsifying capacity, such as its capacity to reduce interfacial tension.

Sunflower oil-water interfacial tension for BC-NF or BC-NC at different concentrations was analyzed. Fig. 3 shows the morphology of the drops and the projection of the behavior of BC-NF or BC-NC at the oil/water interface, as a function of nanocellulose concentration. As expected, interfacial tension decreased with increasing nanocellulose (BC-NF or BC-NC) concentration. At the studied concentrations, the interfacial tension was not statistically different for both nanocelluloses. Recent studies have shown that the adsorption capacity of BC-NFs with a carboxylate group content at 0.01 % (the sample used in this work has 12 % oxidation) in a suspension droplet at the dodecane (density 0.75 g/mL (Thompson et al., 2015)) interface with water was able to reduce the interfacial tension to 42.5–52.5 mN/m (Wu et al., 2021). In this study, 0.5 % of BC-NF or BC-NC, was able to reduce the tension at the oil-water interface to 25.06 ± 0.44 or 24.59 ± 0.30 mN/m, respectively. A low concentration of nanocellulose can exhibit effective adsorption behavior at the oil-water interface, attributed to both, charged groups and morphological characteristics. However, besides the nanocellulose concentration, physical properties (such as density, and viscosity) between the dispersed and continuous phases can also influence the stability behavior of an emulsion (K. Zhang et al., 2024). In general, similar physical properties imply a slower creaming rate compared to O/W droplets of the same average size (Dickinson, 2019). In this context, the behavior of BC-NF or BC-NC at the interface with isohexadecane, a dispersed phase of lower density (0.79 g/mL, T = 20 °C), allows for a better assessment of the performance of the new proposed systems (Martins et al., 2020). Fig. 3b shows lower interfacial tension with sunflower oil for both nanocelluloses, suggesting that the aqueous suspensions of BC-NF and BC-NC may have densities closer to sunflower oil (0.92 g/mL) compared to isohexadecane. These results are consistent with previous studies (Martins et al., 2020; Wu et al., 2021).

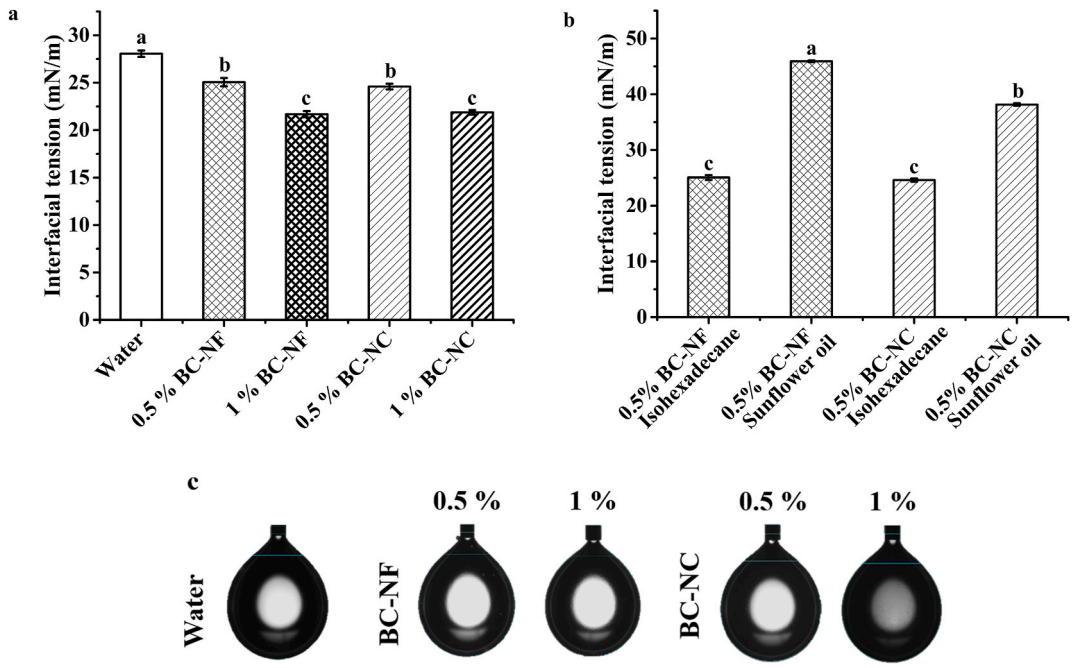


Fig. 3. (a) Interfacial tension of the sunflower oil-water interface at different concentrations of BC-NF or BC-NC. (b) Interfacial tension of the sunflower oil-water or isohexadecane oil-water, at a concentration of 0.5 % BC-NF or BC-NC. (c) Illustration of BC-NF or BC-NC surfactant film formation at the sunflower oil-water interface using the pendant drop method. Values reported are the means (n = 3). Values followed by at least one common letter are not significantly different ($p > 0.05$).

4.4. Pickering emulsions

4.4.1. Physico-chemical characterization

In this work, studies were conducted to examine the effect of charged BC (BC-NF or BC-NC) and salt concentration on droplet size, stability at room temperature (freshly prepared or after 30 days of storage) or towards centrifugal forces, and the rheology of Pickering emulsions with low-oil content. The structuring of BC in emulsion droplets was observed using Cryo-SEM and CLSM.

Cryo-SEM image (Fig. 4a) shows the nanocellulose on the surface of emulsion droplets. BC-NC appeared capable of adsorbing in layers as Pickering stabilizers in the interface of low-oil (1 %) emulsions. Each droplet is surrounded by a continuous layer of BC-NC, indicating that the oil droplets became localized within the network formed by the arrangement of BC that occurred during emulsification. The cellulose was stained with calcofluor and the oil phase with beta-carotene (Fig. 4b) for CLSM observation. Again, the nanocellulose can be found concentrated on the interface, providing steric hindrance, and stabilizing the oil droplets.

The droplet sizes stabilized by different concentrations of BC-NF or BC-NC are shown in Table 1. The corresponding micrographs after preparation (0 days) or after 30 days of storage at room temperatures (30 days) are displayed in Figs. 5 and 6.

In general, the emulsions displayed a stable behavior (Figs. 5 and 6), and the average size of droplets ranged between values less than 5 μm (1.73–4.13 μm). Similar values were reported for low-oil emulsions (1 % sunflower oil) stabilized by depletion in a dual system containing non-adsorbing CNC (obtained from cotton fiber filter paper and hydrolyzed with sulfuric acid 64 wt %) and CNF (prepared by disintegrating never-dried, fully bleached and fines-free sulfite hardwood (birch) disintegrated through a high-pressure microfluidizer) in the aqueous phase (2.2 ± 0.2 μm) (Bai et al., 2018). We state that the final microstructure of emulsions can be determined by the volumetric fraction of oil to the available Pickering stabilizer, with droplet size controlled by the limited coalescence phenomenon. In other words, the correct balance between the reduced oil fraction and the Pickering stabilizer tends to produce

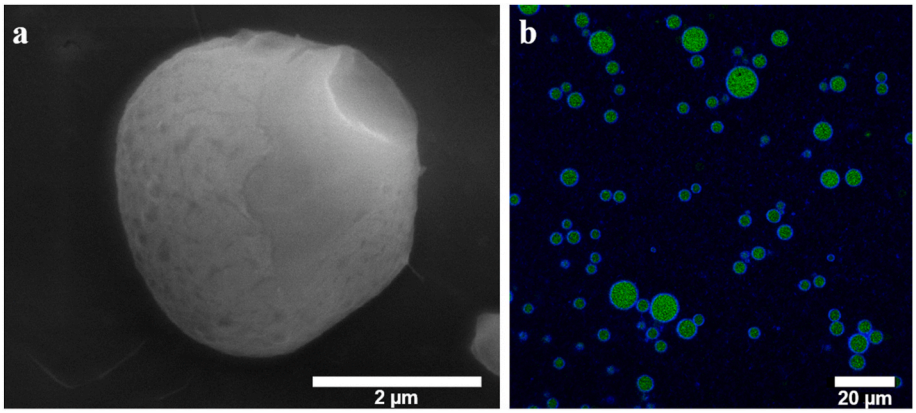


Fig. 4. Cryo-SEM image (a) of a low-oil fraction emulsion (1 %) stabilized with 1 % BC-NC and 50 mM NaCl, and CLSM (b) of a 10 % oil-incorporated emulsion with 0.05 % beta-carotene (green), stabilized with 1 % BC-NC (stained with Calcofluor - blue) and 50 mM NaCl. The image shows an area of 512 × 512 μm from a 4x4 tile scan taken with a 63x magnification objective.

Table 1
Effect of nanocellulose and salt concentration on droplet size of emulsions with low sunflower oil fraction (1 % v/v) over time.

	NaCl (mM)	(0.5 % w/v) Size $D_{(3,2)}$ (μm)		(1 % w/v) Size $D_{(3,2)}$ (μm)	
		0 day	30 days	0 day	30 days
BC-NF	0	2.07 ± 0.13$^{bc,*,\#}$	3.08 ± 0.39*	3.20 ± 0.23$^{b,\#}$	3.22 ± 0.10
	12.5	2.75 ± 0.26^{ab,*}	3.54 ± 0.30*	2.77 ± 0.20^{b}	2.93 ± 0.10
	50	2.90 ± 0.44 $^{a,\#}$	3.01 ± 0.38	4.13 ± 0.31$^{a,\#}$	4.10 ± 0.19
BC-NC	0	1.73 ± 0.17 ^{c,*}	6.20 ± 0.24*	1.77 ± 0.20^{c}	1.97 ± 0.30
	12.5	1.97 ± 0.25 ^{c}	1.89 ± 0.17	2.04 ± 0.26^{c}	2.55 ± 0.54
	50	2.80 ± 0.26 ^{ab}	3.20 ± 0.22	3.06 ± 0.18^{b}	3.17 ± 0.20

The reported values are means ± standard deviation. Values in the same column followed by at least one common lowercase letter are not significantly different ($p > 0.05$). Pairs of values (between 0 and 30 days) followed by * are significantly different from each other (*t*-test, $p \leq 0.05$). Pairs of values (in day 0, between different nanocellulose concentrations) followed by # are significantly different from each other (*t*-test, $p \leq 0.05$).

smaller average droplet sizes, and their formation and stability depend on this equilibrium (Low et al., 2020).

Particularly, emulsions without salt, stabilized with 1 % BC-NF, formed larger droplets compared to droplets stabilized with BC-NC at the same BC concentration. At this point, the influence of the shape and size of BC (short rods or long fibrils) was predominant in affecting the average droplet size. BC-NF has a high aspect ratio and, therefore, may tend to adsorb more slowly at the interface, increasing the final droplet size (Albert et al., 2019). Additionally, short rods of BC-NC can form a denser organization on the droplet surface (Kalashnikova et al., 2013). Overall, the length of nanocellulose can adjust the structure of emulsions, from individual droplets (short nanocellulose) to entangled network structures (long nanocellulose), resulting in distinct stabilization systems (Dai et al., 2020).

When considering the addition of salt, there was an apparent trend for all emulsions which is the increase of the droplet size as the salt concentration is increased from 0 to 50 mM. However, a more prominent significant effect was observed in emulsions stabilized with BC-NC at 50 mM of NaCl. In this case, the droplets formed with 0.5 % BC-NC (2.80 ± 0.26 μm), or 1% BC-NC (3.06 ± 0.18 μm) were 62 % and 73 % larger in size than in emulsions without salt (1.73 ± 0.17 μm and 1.77 ± 0.20 μm, respectively), without compromising stability over 30 days. This trend was also observed in emulsions with a reduced oil fraction, stabilized with vegetal cellulose nanofibrils (CNF) subjected to oxidation mediated by TEMPO/NaOCl/NaBr and non-adsorbing CNF (disintegrated by high-pressure microfluidization) as a depletion agent at different NaCl concentrations: 3.6 μm (0 % weight NaCl), 6.9 μm (0.004 % weight NaCl), and 11.0 μm (0.006 % weight NaCl) (Guo et al., 2022).

4.4.2. Stability

A critical aspect of emulsions regards their stability. Thermodynamically, an emulsion is considered stable when the quantity and size of droplets in the internal phase, per unit volume of the continuous phase, remain consistent over time. This implies that there are no changes in the energy value of the system or its interfacial area.

Both BC-NF and BC-NC were able to form macroscopically stable emulsions at a concentration of 1 %, showing no instability after 30 days of storage at room temperature (Table 1). In this case, both nanocelluloses demonstrated good stability at all tested salt concentrations (0, 12.5, and 50 mM), as confirmed by microscopy (Figs. 5 and 6). On the other hand, emulsions containing 0.5 % BC-NF or BC-NC in the absence of salt experienced a significant increase in the average droplet size from 2.07 ± 0.13 and 1.73 ± 0.17 μm to 3.08 ± 0.39 and 6.20 ± 0.24 μm, respectively. Emulsions containing 0.5 % BC-NC were also accompanied by the formation of a thin cream layer on the surface over 30 days, with coalescing oil droplets, as revealed by microscopic evaluation (Fig. 6). However, at the lowest salt concentration (12.5 mM), 0.5 % BC-NC effectively stabilized the emulsions, forming droplets of 1.97 ± 0.25 μm that remained stable after 30 days (1.89 ± 0.17 μm). In contrast, the stability of emulsions containing 0.5 % BC-NF was achieved in the presence of 50 mM of NaCl.

Low-oil-fraction emulsions are diluted systems, thus representing a set of more dispersed droplets. Therefore, although BC-NF systems generally benefit from the gel network structure formed in the aqueous phase (provided by the high aspect ratio of the nanofibrils) (Bai et al., 2018; Courtenay et al., 2021; Guo et al., 2022), at this concentration (0.5

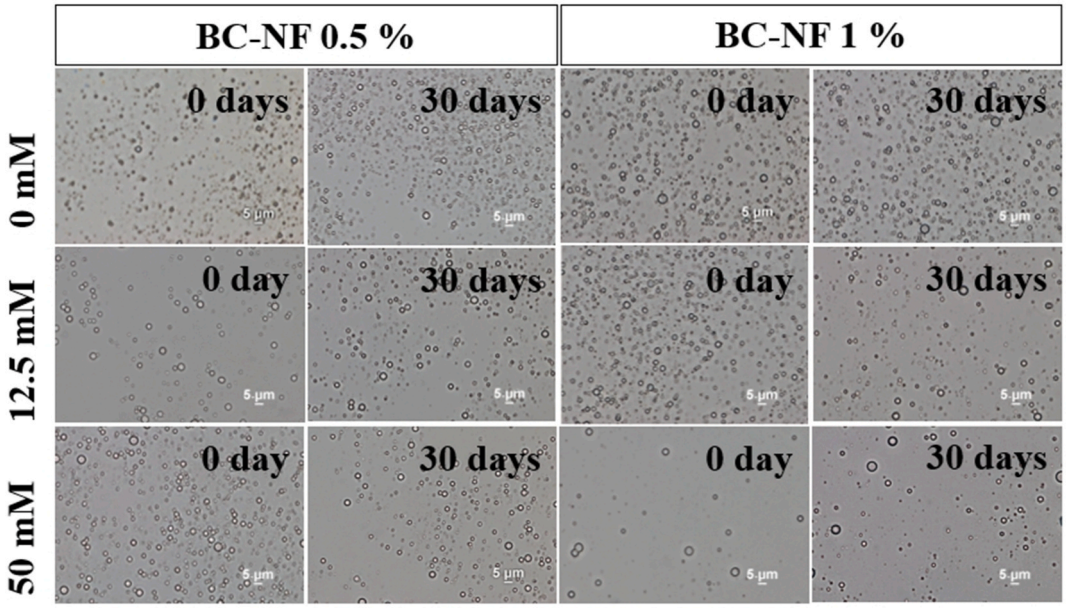


Fig. 5. Optical microscopy ~~and appearance~~ of Pickering emulsions stabilized by BC-NF (0.5 % or 1 % w/v) under different ionic strengths (0, 12.5 and 50 mM) after preparation or after 30 days of storage at room temperature. The scale bar is 5 μm.

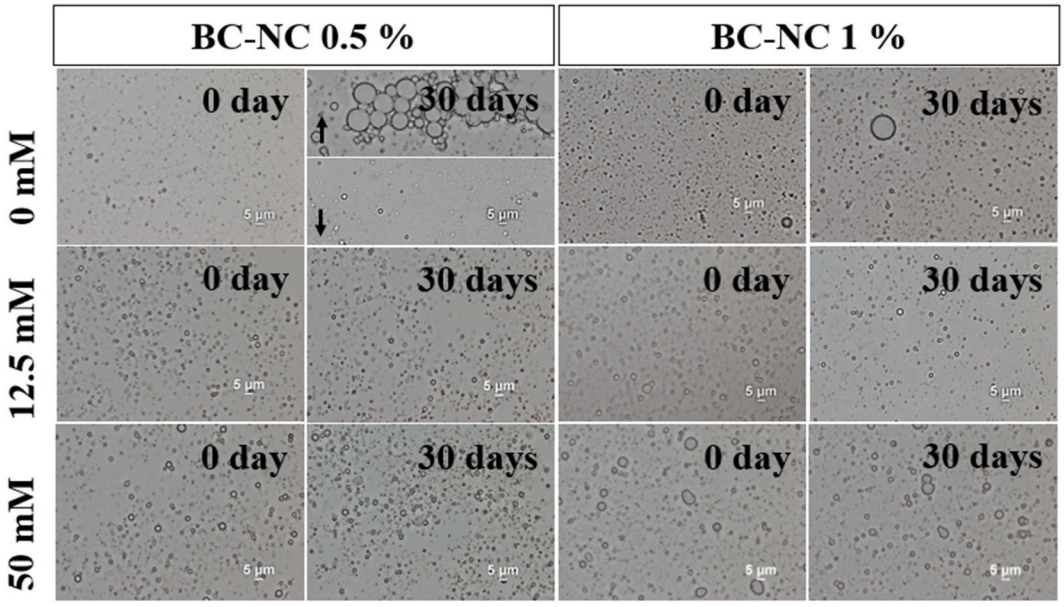


Fig. 6. Optical microscopy of Pickering emulsions stabilized by BC-NC (0.5 % and 1 % w/v) under different ionic strengths (0, 12.5 and 50 mM) after preparation or after 30 days of storage at room temperature. Arrows in the microscopy images indicate upper and lower phases formed. The scale bar is 5 µm.

%), they were not effectively adsorbed in low-oil-fraction systems, where BC-NF was the only stabilizing agent.

On the other hand, emulsions containing higher oil fractions increase the packing fraction of oil droplets and consequently present a smaller hydrodynamic area in the continuous phase (Dickinson & Golding, 1997; Sun & Gunasekaran, 2009). Thus, the role of long fibrils in covering the droplets and filling the continuous phase, even at lower concentrations, can be effective (Goi et al., 2019). Therefore, the diameter of the formed droplets is controlled by the concentration of nanocellulose and its arrangement at the interface, reflecting its stability over time (Schmitt et al., 2014). In this case, the dosage of the stabilizer as a percentage of the oil phase can also be considered (Gestranius et al., 2017).

Under centrifugal force, the systems containing low BC-NF concentration (0.5 %) were not stable (Fig. 7). Under these circumstances, the force applied to the emulsion increased the packing fraction of the oil droplets, reducing the hydrodynamic area in the continuous phase. Under these conditions, the emulsions containing 1 % BC-NF did not exhibit creaming, maintaining their initial appearance. However, in this system, microscopy revealed that the salt-free emulsion was more susceptible to coalescence, while the emulsions with salt maintained individualized droplets (Fig. 7). The presence of salt, therefore, also played an effective role in the emulsions with 1 % BC-NF, promoting the formation of long gel networks for droplet coverage and continuous phase filling against coalescence or flocculation. Thus, the form of bacterial nanocellulose is also a relevant factor in determining the stability of Pickering emulsions.

The systems containing BC-NC were more unstable, accelerating the

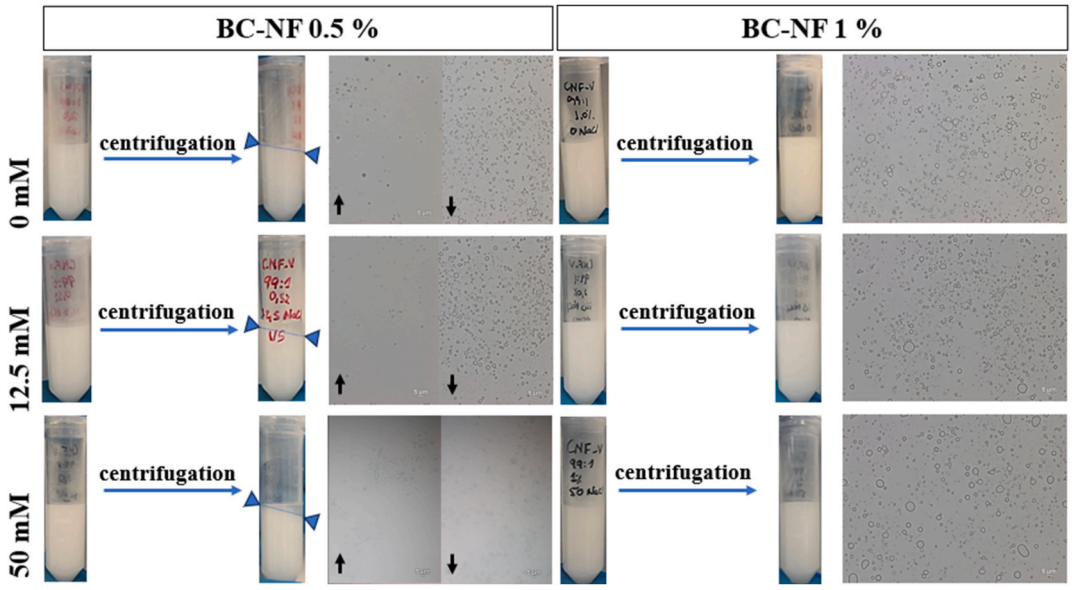


Fig. 7. Images of Pickering emulsions stabilized by BC-NF (0.5 % or 1 % w/v) under different ionic strengths (0, 12.5 and 50 mM) before (30 min after emulsification) and after centrifugation (1520 *g* for 2 min). Optical microscopy was used to evaluate the droplets after centrifugation. Arrows in the microscopy images indicate upper and lower phases formed. The scale bar is 5 µm.

flocculation and coalescence processes of the oil droplets after centrifugation (Fig. 8). For the BC-NC systems containing salt, centrifugation resulted in a creaming phenomenon, concentrating the droplets in the lower phase but without phase separation, suggesting strong adsorption of BC at the O/W interface. This is confirmed by the microscopy images of the cream after centrifugation.

In addition, the presence of surface charges due to the carboxylic groups (BC-NF) or sulfate esters (BC-NC), should be of sufficient density to promote electrostatic repulsion between the nanocellulose particles, while not preventing them from adsorbing in the oil droplet (Boughriba et al., 2021; Wu et al., 2022). When negatively charged nanocellulose moves toward the oil-water interface, which is also negatively charged due to the preferential adsorption of hydroxide ions, significant repulsion occurs. This repulsion can create an energy barrier preventing the adsorption of particles at the droplet interface, which can lead to the formation of a weakly adsorbed or less dense structure around the oil droplets as well reported (Jiménez Saelices & Capron, 2018; Varanasi et al., 2018).

The weakly adsorbed or less dense structure can promote the rearrangement of particles that, given the high surface area of coverage and lower concentration in the medium, tend to organize themselves into new coalesced droplets with a smaller surface area, leading to an increase in their average diameters (Jiménez Saelices & Capron, 2018). Thus, a high surface charge density can inevitably lead to emulsion breakdown by electrostatic repulsion. In emulsions stabilized with 0.5 % of BC-NF or BC-NC, there was an increase in the droplet size over time due to greater mobility of charged particles. In this case, the formation of stable emulsions using low concentrations of nanocellulose is impaired.

On the other hand, 1 % of BC-NF or BC-NC were able to stabilize the emulsions. It can be inferred that an increased concentration leads to a superior coating of the interface and enhanced structuring of the continuous phase, thereby contributing to heightened stability. The formed aggregates have higher adsorption energy that predominates over the repulsion force between the nanocelluloses and the oil-water interface. The adsorbed aggregates minimize the interfacial free energy mainly by reducing the interfacial area between the oil-water interfaces. Therefore, at a concentration of 1 %, nanocelluloses were able to stabilize emulsions with low oil content (Varanasi et al., 2018).

4.4.3. *Effect of adding NaCl*

In systems containing conventional low molecular weight surfactants, the addition of salts reduces the ionic repulsion between the main groups and induces phase transitions, inducing more complex micellar structures. At this point, the electrolytes favor the organization of molecules into spherical micelles that combine to form hexagonal structures, reflecting an increase in viscosity in the system (Cornwell, 2018).

In Pickering emulsions, stabilized with BC-NC, the addition of NaCl also provided a viscosity increase phenomenon observed even macroscopically. As previously stated, when salt is present, surfaces are neutralized and become less hydrophilic. This condition potentially aids the migration of particles to the interface, where they can adsorb and play a role in stabilizing the emulsion. In emulsions with BC-NF, this behavior was not observed macroscopically, but it exhibited a positive rheological response to greater structuring of the nanofibrils at the interface of the droplets of the low-oil emulsions (Wu et al., 2021).

The positioning of NaCl electrolyte counter ions on highly charged bacterial nanocellulose nanoparticles (>|45| mV) was able to reduce electrostatic repulsion, favoring better interactions at the oil-water interface. In addition to the evident increase in viscosity, NaCl also played an important role in the formation and stability of emulsions. In emulsions with 0.5 % BC-NC, the addition of 12.5 mM was able to orient the cellulose nanocrystals on the surface of the oil droplets, reducing the need to increase the concentration of nanocellulose (1 %) to promote enhanced stability (L. Liu et al., 2018; Varanasi et al., 2018). Cryo-SEM microscopy was able to capture the arrangement of BC-NC or BC-NF in emulsions with 0, 12.5, or 50 mM NaCl, evidencing the migration of the nanocellulose towards the surface of oil droplets when NaCl was added (Fig. 9).

In both cases, at a concentration of 50 mM NaCl, the average diameters of the droplets after preparation were increased by 1 μm, where the non-adsorbed nanocellulose undergoes a reduction in electrostatic charge, favoring the deposition of new particles and layer packing at the interface oil-water (F. Liu & Tang, 2016). The size of nanocellulose plays a crucial role in the size of oil droplets. Larger sizes result in larger droplet emulsions. The addition of salt reduces the charge of nanoparticles, consequently decreasing electrostatic repulsion. This leads to nanocelluloses agglomeration, forming network structures that, in turn, interfere with the size of the formed droplets. Although larger droplets are produced, the strong cohesive network formed by nanocellulose

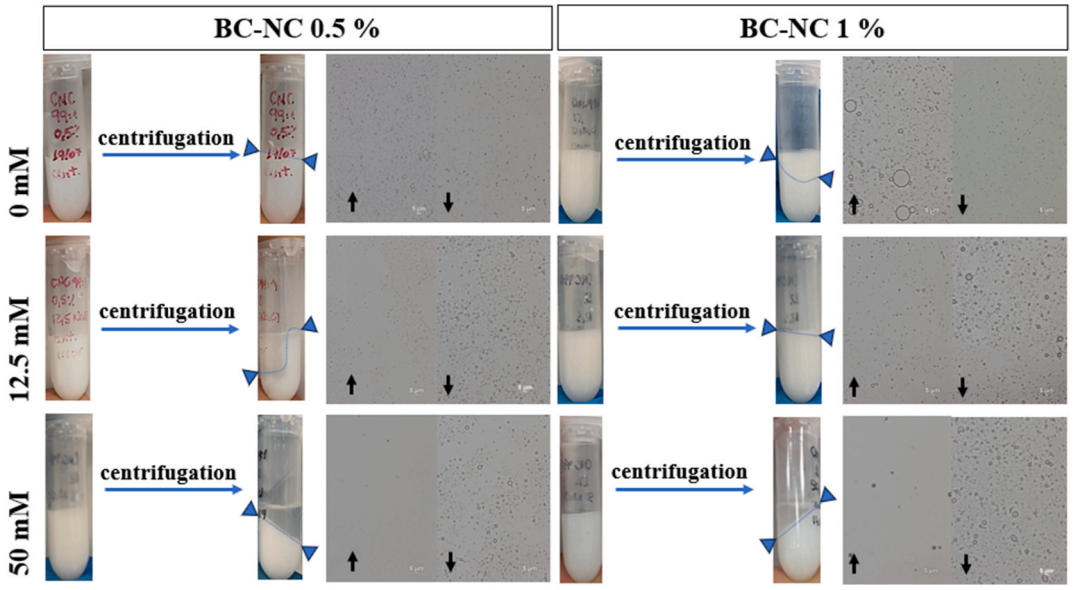


Fig. 8. Images of Pickering emulsions stabilized by BC-NF (0.5 % or 1 % w/v) under different ionic strengths (0, 12.5 and 50 mM) before (30 min after emulsification) and after centrifugation (1520 *g* for 2 min). Optical microscopy was used to evaluate the droplets after centrifugation. Arrows in the microscopy images indicate upper and lower phases formed. The scale bar is 5 μm.

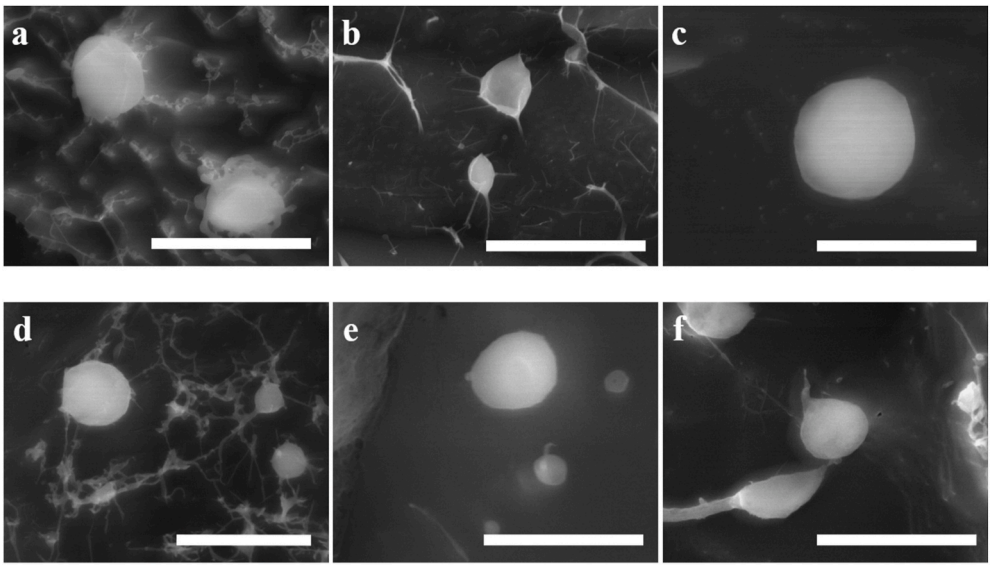


Fig. 9. Cryo-SEM images of 0.5 % BC-NF emulsions (a, b, c) or BC-NC (d, e, f) without salt (a, d), with 12.5 mM (b, e) or 50 mM NaCl (c, f). The scale bars: a – 3 μm, b – 6 μm, c – 2 μm, d – 2 μm, e – 2 μm and f - 2 μm.

aggregation provides robust anchoring at the oil-water interface, as observed by the stability of emulsions over 30 days.

In this case, we possibly obtain a more stable emulsion resistant to breakage and phase separation (Schröder et al., 2018), characterizing it as a model emulsion system with inhibitory behavior of lipid digestion designed for application in low-calorie products, for example (B. Liu et al., 2019). However, the high concentration of NaCl can promote the breakdown of the emulsion due to the marked reduction of charges on the surface of the nanocellulose.

On the other hand, a system containing a low concentration of NaCl may be preferential, as a health claim. Therefore, when the addition of salt is not desirable, considering the use of a higher concentration of nanocellulose becomes relevant for formulation decisions.

4.5. Rheology

Fig. 10 shows the viscosity of the emulsions as a function of the shear rates of Pickering emulsions stabilized by BC-NF or BC-NC. From the rheological curve, the emulsions exhibited a non-Newtonian behavior, which manifested as a shear-thinning property. Previous studies indicated that when the shear rate increases gradually, the droplet network of the emulsion is destroyed by the shear force, reflected in a viscosity decrease (Jia et al., 2019).

Fig. 10 also shows that the apparent viscosity of the Pickering emulsions increased with the addition of NaCl. The reason for this might be the amphiphilic properties of the bacterial nanocellulose, derived from their hydroxyl and carboxyl groups, and crystalline organization along with extensive hydrogen bonding of polymer chains (Zuppolini et al., 2022), and the ionic strength that could influence the charge density and size of BC-NF or BC-NC. Yan et al. (2017) (Yan et al., 2017), observed that with increasing ionic strength from 0 to 200 mM of NaCl, the zeta potential and size of bacterial cellulose nanocrystals gradually increased due to the electrostatic shielding effect and subsequent aggregation effect caused by the addition of NaCl (Chenglin et al., 2012). These authors observed that the addition of NaCl induced the electrostatic shielding of the charged bacterial cellulose and BC-NC via the counterions (Na^+) (Wen et al., 2014). By comparison, BC-NF underwent a higher viscosity increase in response to the ionic strength than BC-NC, indicating better colloidal properties. To explore this effect, the experimental results were adjusted to the Carreau model and non-linear regression, and the corresponding fitting parameters are shown in Tables 2 and 3.

The Carreau model fitted to the experimental data with good accuracy ($R^2adj>0.95$) for both nanocelluloses (BC-NF and BC-NC). This model has been applied to describe the flow behavior of oil-in-water emulsions (Daniel-da-Silva et al., 2011; W. Xu et al., 2021). Pickering

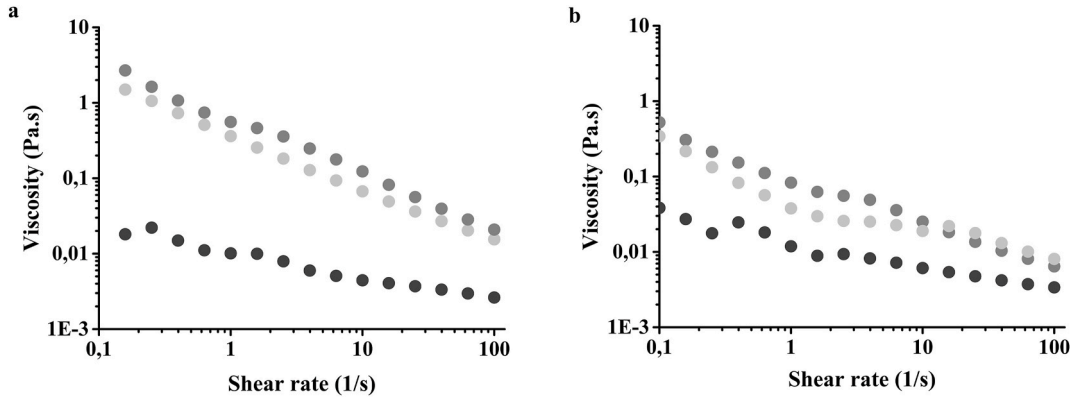


Fig. 10. Viscosity as a function of shear rate for emulsions composed of 0.5 % of BC-NF (a) or BC-NC (b) without salt (NaCl) (●) or with different NaCl concentrations of 12.5 mM (●) and 50 mM (●).

Table 2
Modeling of the flow curve using the Carreau model (Eq. (2)) for Pickering emulsions composed of cellulose nanofibrils (BC-NF).

	BC-NF		
Parameters	0 mM NaCl	12.5 mM NaCl	50 mM NaCl
η_0	0.08 ± 0.03^b	78 ± 17^a	117 ± 62^a
η_∞	0.002 ± 0.0004^a	0.003 ± 0.0001^a	0.002 ± 0.001^a
$\dot{\gamma}_c$	1.8 ± 0.5^a	1393 ± 58^b	969 ± 59^c
N	0.42 ± 0.02^a	0.23 ± 0.02^b	0.25 ± 0.05^b
R^2adj	0.9745	0.9996	0.9973

Values reported are the means ± standard deviations (n = 3). Values in the same row followed by at least one common letter are not significantly different ($p > 0.05$).

Table 3
Modeling of the flow curve using the Carreau model (Eq. (2)) for Pickering emulsions composed of cellulose nanocrystals (BC-NC).

	BC-NC		
Parameters	0 mM NaCl	12.5 mM NaCl	50 mM NaCl
η_0	0.09 ± 0.08^a	7 ± 1^b	4.8 ± 0.9^b
η_∞	0.001 ± 0.0003^a	0.001 ± 0.0003^a	0.005 ± 0.001^b
$\dot{\gamma}_c$	375.9 ± 0.4^a	1213.03 ± 141^b	1604.1 ± 93^c
N	0.58 ± 0.02^a	0.388 ± 0.01^b	0.424 ± 0.07^c
R^2adj	0.9686	0.9951	0.9545

Values reported are the means ± standard deviations (n = 3). Values in the same row followed by at least one common letter are not significantly different ($p > 0.05$).

emulsions composed of BC-NF show an increase of η_0 values with an increase in salt concentration, and this behavior can be due to decreasing water content. The increase of salt affects the polymer conformation and usually, a higher η_0 is correlated with a strong conformation. This effect is more evident in Pickering emulsions composed of BC-NF when compared with BC-NC, consistent with results from Courtenay et al., 2021. This behavior was attributed to the repulsive force between the nanofibrils resulting from their charge density and high aspect ratio, leading to a lower agglomeration capacity and lower friction. Furthermore, it is possible to observe that relaxation times ($\dot{\gamma}_c$) are shorter for BC-NF and BC-NC emulsions, without NaCl, which is related to the emulsion instability (creaming). Increasing the salt concentration makes it possible to observe an increase in $\dot{\gamma}_c$, suggesting an enhancement of interactions between noncovalent interactions. It was also observed that the values of η_∞ were lower than 0.01 which is in accordance with the results reported by other authors (Tang et al., 2021). In this study, all the emulsions tested exhibited shear thinning (pseudoplastic) behavior as evidenced by their N values lower than 1.0. Nanoparticles effectively reduced the interfacial tension. The morphological properties and concentration of nanocellulose had a significant effect on the emulsifying capacity. Under the same dosage of cellulose, BC-NF displayed the best emulsifying capacity.

5. Conclusion

The potential use of bacterial nanocellulose (nanocrystals or nanofibrils) as a stabilizer in Pickering emulsions with low oil content was evaluated. Nanofibrils (BC-NF) were produced through mechanical defibrillation of TEMPO-mediated oxidized bacterial cellulose and nanocrystals (BC-NC) through sulfuric acid hydrolysis. Both nanocelluloses exhibited high surface charge (>|45| mV) and great hydrophilicity (contact angle around 30° for both).

After the production of Pickering emulsions, we observed the effect of nanocellulose and salt concentrations on interfacial tension, size, stability, and rheology. When increasing the nanocellulose concentration, the interfacial tension is reduced. Higher stability was observed for high salt and nanocellulose concentrations. For emulsions stabilized by BC-NC, lower cellulose concentration combined with low salt concentrations proved to be sufficient for a total stabilization of the droplets. Cryo-SEM and confocal microscopy images show the nanocellulose location at the oil-water interface. From a rheological perspective, the addition of NaCl causes an increase in viscosity, which was more pronounced in the BC-NF samples. These results indicate that the use of BC-NF or BC-NC, along with salt, allows for tuning the emulsion properties for specific applications, such as entrapping oil droplets in distinct systems designed for the formulation of low-fat food products.

Funding

The author Ana Isabel Bourbon acknowledges FCT funding, through the individual scientific employment program contract (2020.03447.CEECIND). The authors Morsyleide de Freitas Rosa and Náyra de Oliveira Frederico Pinto acknowledges funding by FCT/CAPES 99999.008530/2014–09.

CRediT authorship contribution statement

Náyra O.F. Pinto: Writing – review & editing, Writing – original draft, Visualization, Validation, Investigation, Formal analysis, Data curation. **Ana Isabel Bourbon:** Writing – review & editing, Writing – original draft, Methodology, Formal analysis, Conceptualization. **Daniela Martins:** Writing – review & editing, Methodology. **André Pereira:** Writing – review & editing, Visualization. **Miguel A. Cerqueira:** Writing – review & editing, Conceptualization. **Lorenzo Pastrana:** Resources, Project administration. **Miguel Gama:** Writing – review & editing, Resources, Conceptualization. **Henriette M.C. Azeredo:** Writing – review & editing, Conceptualization. **Morsyleide F. Rosa:** Writing – review & editing, Resources, Conceptualization. **Catarina Gonçalves:** Writing – review & editing, Writing – original draft, Supervision, Methodology, Funding acquisition, Conceptualization.

Declaration of competing interest

The authors declare that they have no known competing financial interests or personal relationships that could have appeared to influence the work reported in this paper.

Data availability

Data will be made available on request.

Appendix A. Supplementary data

Supplementary data to this article can be found online at https://doi.org/10.1016/j.foodhyd.2024.110427.

References

Ajkidkarn, P., & Manuspiya, H. (2020). Novel bacterial cellulose nanocrystals/polyether block amide microporous membranes as separators for lithium-ion batteries. *International Journal of Biological Macromolecules, 164*, 3580–3588. https://doi.org/10.1016/j.ijbiomac.2020.08.234

Albert, C., Beladjine, M., Tsapis, N., Fattal, E., Agnely, F., & Huang, N. (2019). Pickering emulsions: Preparation processes, key parameters governing their properties and potential for pharmaceutical applications. In *Journal of controlled release* (Vol. 309, pp. 302–332). Elsevier B.V. https://doi.org/10.1016/j.jconrel.2019.07.003.

Andrade, F. K., Morais, J. P. S., Muniz, C. R., Nascimento, J. H. O., Vieira, R. S., Gama, F. M. P., & Rosa, M. F. (2019). Stable microfluidized bacterial cellulose suspension. *Cellulose, 26*, 5851–5864. https://doi.org/10.1007/s10570-019-02512-y

Anjali, T. G., & Basavaraj, M. G. (2018). Influence of pH and salt concentration on Pickering emulsions stabilized by colloidal peanuts. *Langmuir, 34*, 13312–13321. https://doi.org/10.1021/acs.langmuir.8b02913

Arserim-Uçar, D. K., Korel, F., Liu, L. S., & Yam, K. L. (2021). Characterization of bacterial cellulose nanocrystals: Effect of acid treatments and neutralization. *Food Chemistry, 336*. https://doi.org/10.1016/j.foodchem.2020.127597. Article 127597.

Azeredo, H. M. C., Barud, H., Farinas, C. S., Vasconcellos, V. M., & Claro, A. M. (2019). Bacterial cellulose as a raw material for food and food packaging applications. In *Frontiers in sustainable food systems* (Vol. 3)Frontiers Media S.A. https://doi.org/10.3389/fsufs.2019.00007. Article 7.

Bago Rodriguez, A. M., & Binks, B. P. (2022). High internal phase Pickering emulsions. In *Current opinion in colloid and interface science* (Vol. 57)Elsevier Ltd. https://doi.org/10.1016/j.cocis.2021.101556. Article 101556.

Bai, L., Huan, S., Rojas, O. J., & McClements, D. J. (2021). Recent innovations in emulsion science and technology for food applications. *Journal of Agricultural and Food Chemistry, 69*, 8944–8963. https://doi.org/10.1021/acs.jafc.1c01877

Bai, L., Huan, S., Xiang, W., & Rojas, O. J. (2018). Pickering emulsions by combining cellulose nanofibrils and nanocrystals: Phase behavior and depletion stabilization. *Green Chemistry, 20*, 1571–1582. https://doi.org/10.1039/c8gc00134k

Bao, Y., Xue, H., Yue, Y., Wang, X., Yu, H., & Piao, C. (2021). Preparation and characterization of pickering emulsions with modified okara insoluble dietary fiber. *Foods, 10*. https://doi.org/10.3390/foods10122982. Article 2982.

Binks, B. P., & Lumsdon, S. O. (2000). Influence of particle wettability on the type and stability of surfactant-free emulsions. *Langmuir, 16*, 8622–8631. https://doi.org/10.1021/la000189s

Boughriba, S., Souissi, N., Nasri, R., Nasri, M., & Li, S. (2021). pH sensitive composite hydrogels based on gelatin and reinforced with cellulose microcrystals: In depth physicochemical and microstructural analyses for controlled release of vitamin B2. *Materials Today Communications, 27*. https://doi.org/10.1016/j.mtcomm.2021.102334. Article 102334.

Cai, Z., Wei, Y., Shi, A., Zhong, J., Rao, P., Wang, Q., & Zhang, H. (2023). Correlation between interfacial layer properties and physical stability of food emulsions: Current trends, challenges, strategies, and further perspectives. In *Advances in colloid and interface science* (Vol. 313)Elsevier B.V. https://doi.org/10.1016/j.cis.2023.102863. Article 102863.

Chassaing, B., Koren, O., Goodrich, J. K., Poole, A. C., Srinivasan, S., Ley, R. E., & Gewirtz, A. T. (2015). Dietary emulsifiers impact the mouse gut microbiota promoting colitis and metabolic syndrome. *Nature, 519*, 92–96. https://doi.org/10.1038/nature14232

Chenglin, Y., Yiqun, Y., Ye, Z., Na, L., Xiaoya, L., Jing, L., & Ming, J. (2012). Self-assembly and emulsification of poly{[styrene-alt-maleic acid]-co-[styrene-alt-(N-3,4-dihydroxyphenylethyl-maleamic acid)]. *Langmuir, 28*, 9211–9222. https://doi.org/10.1021/la301605a

Chuberre, B., Araviiskaia, E., Bieber, T., & Barbaud, A. (2019). Mineral oils and waxes in cosmetics: An overview mainly based on the current European regulations and the safety profile of these compounds. In *Journal of the European academy of dermatology and venereology* (Vol. 33, pp. 5–14). Blackwell Publishing Ltd. https://doi.org/10.1111/jdv.15946.

Cornwell, P. A. (2018). A review of shampoo surfactant technology: Consumer benefits, raw materials and recent developments. In *International journal of cosmetic science* (Vol. 40, pp. 16–30). Blackwell Publishing Ltd. https://doi.org/10.1111/ics.12439.

Courtenay, J. C., Jin, Y., Schmitt, J., Hossain, K. M. Z., Mahmoudi, N., Edler, K. J., & Scott, J. L. (2021). Salt-responsive Pickering emulsions stabilized by functionalized cellulose nanofibrils. *Langmuir, 37*, 6864–6873. https://doi.org/10.1021/acs.langmuir.0c03306

Cox, S., Sandall, A., Smith, L., Rossi, M., & Whelan, K. (2021). Food additive emulsifiers: A review of their role in foods, legislation and classifications, presence in food supply, dietary exposure, and safety assessment. In *Nutrition reviews* (Vol. 79, pp. 726–741). Oxford University Press. https://doi.org/10.1093/nutrit/nuaa038.

Dai, H., Wu, J., Zhang, H., Chen, Y., Ma, L., Huang, H., Huang, Y., & Zhang, Y. (2020). Recent advances on cellulose nanocrystals for Pickering emulsions: Development and challenge. In *Trends in food science and technology* (Vol. 102, pp. 16–29). Elsevier Ltd. https://doi.org/10.1016/j.tifs.2020.05.016.

Daniel-da-Silva, A. L., Ferreira, L., Gil, A. M., & Trindade, T. (2011). Synthesis and swelling behavior of temperature responsive κ-carrageenan nanogels. *Journal of Colloid and Interface Science, 355*, 512–517. https://doi.org/10.1016/j.jcis.2010.12.071

Dickinson, E. (2019). Particle-based stabilization of water-in-water emulsions containing mixed biopolymers. In *Trends in food science and technology* (Vol. 83, pp. 31–40). Elsevier Ltd. https://doi.org/10.1016/j.tifs.2018.11.004.

Dickinson, E., & Golding, M. (1997). Rheology of sodium caseinate stabilized oil-in-water emulsions. *Journal of Colloid and Interface Science, 191*, 166–176.

do Nascimento, E. S., Pereira, A. L. S., Barros, M. de O., Barroso, M. K. de A., Lima, H. L. S., Borges, M. de F., Feitosa, J. P. de A., de Azeredo, H. M. C., & Rosa, M. de F. (2019). TEMPO oxidation and high-speed blending as a combined approach to disassemble bacterial cellulose. *Cellulose, 26*, 2291–2302. https://doi.org/10.1007/s10570-018-2208-2

Ford Kraft Foods, L. D., Raju Borwankar, U. P., Pechak, D., & Schwimmer, B. (2004). Dressings and sauces. In S. E. Friberg, K. Larsson, & J. Sjoblom (Eds.), *Food emulsions fourth edition, revised and expanded*. Marcel Dekker, Inc.

Fujisawa, S., Togawa, E., & Kuroda, K. (2017). Nanocellulose-stabilized Pickering emulsions and their applications. In *Science and technology of advanced materials* (Vol. 18, pp. 959–971). Taylor and Francis Ltd. https://doi.org/10.1080/14686996.2017.1401423.

Gao, Y., Lin, D., Peng, H., Zhang, R., Zhang, B., & Yang, X. (2023). Low oil Pickering emulsion gels stabilized by bacterial cellulose nanofiber/soybean protein isolate: An excellent fat replacer for ice cream. *International Journal of Biological Macromolecules, 247*, Article 125623. https://doi.org/10.1016/j.ijbiomac.2023.125623

Gestranius, M., Stenius, P., Kontturi, E., Sjöblom, J., & Tammelin, T. (2017). Phase behaviour and droplet size of oil-in-water Pickering emulsions stabilised with plant-derived nanocellulosic materials. *Colloids and Surfaces A: Physicochemical and Engineering Aspects, 519*, 60–70. https://doi.org/10.1016/j.colsurfa.2016.04.025

Goi, Y., Fujisawa, S., Saito, T., Yamane, K., Katsushi, K., & Isogai, A. (2019). Dual functions of TEMPO-oxidized cellulose nanofibers in oil-in-water emulsions: A pickering emulsifier and a unique dispersion stabilizer. *Langmuir, 35*, 10920–10926. https://doi.org/10.1021/acs.langmuir.9b01977

Guo, S., Bai, L., Li, J., Bi, R., Huan, S., & Rojas, O. J. (2022). Depletion effects and stabilization of Pickering emulsions prepared from a dual nanocellulose system. *ACS Sustainable Chemistry & Engineering, 10*, 9066–9076. https://doi.org/10.1021/acssuschemeng.2c01059

Hedayati, S., Shahidi, F., Koocheki, A., Farahnaky, A., & Majzoobi, M. (2020). Influence of pregelatinized and granular cold water swelling maize starches on stability and physicochemical properties of low fat oil-in-water emulsions. *Food Hydrocolloids, 102*. https://doi.org/10.1016/j.foodhyd.2019.105620. Article 105620.

Hu, Y., Qiu, C., Jin, Z., Qin, Y., Zhan, C., Xu, X., & Wang, J. (2020). Pickering emulsions with enhanced storage stabilities by using hybrid β-cyclodextrin/short linear glucan nanoparticles as stabilizers. *Carbohydrate Polymers, 229*, Article 115418. https://doi.org/10.1016/j.carbpol.2019.115418

Huang, L., Xu, C., Gao, W., Rojas, O. J., Jiao, W., Guo, S., & Li, J. (2024). Formulation and stabilization of high internal phase emulsions via mechanical cellulose nanofibrils/ethyl lauroyl arginate complexes. *Carbohydrate Polymers, 324*, Article 121541. https://doi.org/10.1016/j.carbpol.2023.121541

Jia, Y., Zhai, X., Fu, W., Liu, Y., Li, F., & Zhong, C. (2016). Surfactant-free emulsions stabilized by tempo-oxidized bacterial cellulose. *Carbohydrate Polymers, 151*, 907–915. https://doi.org/10.1016/j.carbpol.2016.05.099

Jia, Y., Zheng, M., Xu, Q., & Zhong, C. (2019). Rheological behaviors of Pickering emulsions stabilized by TEMPO-oxidized bacterial cellulose. *Carbohydrate Polymers, 215*, 263–271. https://doi.org/10.1016/j.carbpol.2019.03.073

Jiang, H., Sheng, Y., & Ngai, T. (2020). Pickering emulsions: Versatility of colloidal particles and recent applications. In *Current opinion in colloid and interface science* (Vol. 49, pp. 1–15). Elsevier Ltd. https://doi.org/10.1016/j.cocis.2020.04.010.

Jiménez Saelices, C., & Capron, I. (2018). Design of Pickering micro- and nanoemulsions based on the structural characteristics of nanocelluloses. *Biomacromolecules, 19*, 460–469. https://doi.org/10.1021/acs.biomac.7b01564

Kalashnikova, I., Bizot, H., Bertoncini, P., Cathala, B., & Capron, I. (2013). Cellulosic nanorods of various aspect ratios for oil in water Pickering emulsions. *Soft Matter, 9*, 952–959. https://doi.org/10.1039/c2sm26472b

Kalashnikova, I., Bizot, H., Cathala, B., & Capron, I. (2011). New pickering emulsions stabilized by bacterial cellulose nanocrystals. *Langmuir, 27*, 7471–7479. https://doi.org/10.1021/la200971f

Kedzior, S. A., Gabriel, V. A., Dubé, M. A., & Cranston, E. D. (2021). Nanocellulose in emulsions and heterogeneous water-based polymer systems: A review. In *Advanced materials* (Vol. 33)John Wiley and Sons Inc. https://doi.org/10.1002/adma.202002404.

Khan, H., Kadam, A., & Dutt, D. (2020). Studies on bacterial cellulose produced by a novel strain of Lactobacillus genus. *Carbohydrate Polymers, 229*, Article 115513. https://doi.org/10.1016/j.carbpol.2019.115513

Koshani, R., & Madadlou, A. (2018). A viewpoint on the gastrointestinal fate of cellulose nanocrystals. In *Trends in food science and technology* (Vol. 71, pp. 268–273). Elsevier Ltd. https://doi.org/10.1016/j.tifs.2017.10.023.

Li, Q., Huang, Y., Du, Y., Chen, Y., Wu, Y., Zhong, K., Huang, Y., & Gao, H. (2022). Food-grade olive oil Pickering emulsions stabilized by starch/β-cyclodextrin complex nanoparticles: Improved storage stability and regulatory effects on gut microbiota. *Lebensmittel-Wissenschaft & Technologie, 155*. https://doi.org/10.1016/j.lwt.2021.112950. Article 112950.

Li, M. C., Wu, Q., Song, K., Lee, S., Qing, Y., & Wu, Y. (2015). Cellulose nanoparticles: Structure-morphology-rheology relationships. *ACS Sustainable Chemistry & Engineering, 3*, 821–832. https://doi.org/10.1021/acssuschemeng.5b00144

Liu, L., Hu, Z., Sui, X., Guo, J., Cranston, E. D., & Mao, Z. (2018). Effect of counterion choice on the stability of cellulose nanocrystal Pickering emulsions. *Industrial & Engineering Chemistry Research, 57*, 7169–7180. https://doi.org/10.1021/acs.iecr.8b01001

Liu, L., Ode Boni, B. O., Ullah, M. W., Qi, F., Li, X., … Yang, G. (2022). Cellulose: A promising and versatile Pickering emulsifier for healthy foods. *Food Reviews International, 39*, 7081–7111. https://doi.org/10.1080/87559129.2022.2142940

Liu, Z., Lin, D., Shen, R., & Yang, X. (2021). Bacterial cellulose nanofibers improved the emulsifying capacity of soy protein isolate as a stabilizer for pickering high internal-phase emulsions. *Food Hydrocolloids, 112*. https://doi.org/10.1016/j.foodhyd.2020.106279. Article 106279.

Liu, F., & Tang, C. H. (2016). Soy glycinin as food-grade Pickering stabilizers: Part. II. Improvement of emulsification and interfacial adsorption by electrostatic screening. *Food Hydrocolloids, 60*, 620–630. https://doi.org/10.1016/j.foodhyd.2015.10.024

Liu, B., Zhu, Y., Tian, J., Guan, T., Li, D., Bao, C., Norde, W., Wen, P., & Li, Y. (2019). Inhibition of oil digestion in Pickering emulsions stabilized by oxidized cellulose nanofibrils for low-calorie food design. *RSC Advances, 9*, 14966–14973. https://doi.org/10.1039/c9ra02417d

Low, L. E., Siva, S. P., Ho, Y. K., Chan, E. S., & Tey, B. T. (2020). Recent advances of characterization techniques for the formation, physical properties and stability of Pickering emulsion. In *Advances in colloid and interface science* (Vol. 277)Elsevier B.V. https://doi.org/10.1016/j.cis.2020.102117. Article 102117.

Martins, D., Estevinho, B., Rocha, F., Dourado, F., & Gama, M. (2020). A dry and fully dispersible bacterial cellulose formulation as a stabilizer for oil-in-water emulsions. *Carbohydrate Polymers, 230*. https://doi.org/10.1016/j.carbpol.2019.115657. Article 115657.

Maruyama, S., Streletskaya, N. A., & Lim, J. (2021). Clean label: Why this ingredient but not that one? *Food Quality and Preference, 87*. https://doi.org/10.1016/j.foodqual.2020.104062. Article 104062.

McClements, D. J. (2012). Nanoemulsions versus microemulsions: Terminology, differences, and similarities. *Soft Matter, 8*, 1719–1729. https://doi.org/10.1039/c2sm06903b

McClements, D. J. (2015). Reduced-fat foods: The complex science of developing diet-based strategies for tackling overweight and obesity. *Advances in Nutrition, 6*(3), 338S–352S. https://doi.org/10.3945/an.114.006999

Mikulcová, V., Urbánková, L., Kašpárková, V., & Bordes, R. (2023). On the stabilization of emulsions by cellulose nanocrystals and nanofibrils: Interfacial behavior and synergism. *Colloids and Surfaces A: Physicochemical and Engineering Aspects, 675*. https://doi.org/10.1016/j.colsurfa.2023.131975. Article 131975.

Ming, L., Wu, H., Liu, A., Naeem, A., Dong, Z., Fan, Q., Zhang, G., Liu, H., & Li, Z. (2023). Evolution and critical roles of particle properties in pickering emulsion: A review. In *Journal of molecular liquids* (Vol. 388)Elsevier B.V. https://doi.org/10.1016/j.molliq.2023.122775. Article 122775.

Mohiuddin, A. K. (2019). Skin care creams: Formulation and use. *Dermatology Clinics & Research DCR, 5*, 238–271. https://ospublishers.com/pdf/JCT-1-103.pdf.

Morais, J. P. S., Rosa, M. de F., Brito, E. S. de, Azeredo, H. M. C. de, & Figueirêdo, M. C. B. de (2023). Sustainable Pickering emulsions with nanocellulose: Innovations and challenges. In *Foods* (Vol. 12)Multidisciplinary Digital Publishing Institute (MDPI). https://doi.org/10.3390/foods12193599. Article 3599.

Mota, R., Rodrigues, A. C., Silva-Carvalho, R., Costa, L., Martins, D., Sampaio, P., Dourado, F., & Gama, M. (2022). Tracking bacterial nanocellulose in animal tissues by fluorescence microscopy. *Nanomaterials, 12*. https://doi.org/10.3390/nano12152605. Article 2605.

Moustafa, H., Nasr, H. E., & Youssef, A. M. (2022). Development of antibacterial carboxymethyl cellulose/quaternized starch bionanocomposites based on cinnamon essential oil nanoemulsion for wound healing applications. *Biomass Conversion and Biorefinery*. https://doi.org/10.1007/s13399-022-03403-2

Naimi, S., Viennois, E., Gewirtz, A. T., & Chassaing, B. (2021). Direct impact of commonly used dietary emulsifiers on human gut microbiota. *Microbiome, 9*. https://doi.org/10.1186/s40168-020-00996-6. Article 66.

Pandi, N., Sonawane, S. H., & Anand Kishore, K. (2021). Synthesis of cellulose nanocrystals (CNCs) from cotton using ultrasound-assisted acid hydrolysis. *Ultrasonics Sonochemistry, 70*. https://doi.org/10.1016/j.ultsonch.2020.105353. Article 105353.

Parajuli, S., & Ureña-Benavides, E. E. (2022). Fundamental aspects of nanocellulose stabilized Pickering emulsions and foams. In *Advances in colloid and interface science* (Vol. 299)Elsevier B.V. https://doi.org/10.1016/j.cis.2021.102530. Article 102530.

Paximada, P., Tsouko, E., Kopsahelis, N., Koutinas, A. A., & Mandala, I. (2016). Bacterial cellulose as stabilizer of o/w emulsions. *Food Hydrocolloids, 53*, 225–232. https://doi.org/10.1016/j.foodhyd.2014.12.003

Pereira, A. L. S., Feitosa, J. P. A., Morais, J. P. S., & Rosa, M. de F. (2020). Bacterial cellulose aerogels: Influence of oxidation and silanization on mechanical and absorption properties. *Carbohydrate Polymers, 250*. https://doi.org/10.1016/j.carbpol.2020.116927. Article 116927.

Pinto, N. de O. F., Rodrigues, T. H. S., Pereira, R. de C. A., Silva, L. M. A.e., Cáceres, C. A., Azeredo, H. M. C. de, Muniz, C. R., Brito, E. S. de, & Canuto, K. M. (2016). Production and physico-chemical characterization of nanocapsules of the essential oil from Lippia sidoides Cham. *Industrial Crops and Products, 86*, 279–288. https://doi.org/10.1016/j.indcrop.2016.04.013

Rao, M. (2014). Flow and functional models for rheological properties of fluid foods. In *Rheology of Fluid, Semisolid, and Solid Foods. Food Engineering Series*. Boston, MA: Springer. https://doi.org/10.1007/978-1-4614-9230-6_2.

Rhodes, J. M. (2021). Conference on diet and digestive disease plenary lecture 1: Nutrition and gut health: The impact of specific dietary components-its not just five-a-day. *Proceedings of the Nutrition Society, 80*, 9–18. https://doi.org/10.1017/S0029665120000026

Schmitt, V., Destribats, M., & Backov, R. (2014). Colloidal particles as liquid dispersion stabilizer: Pickering emulsions and materials thereof. In *Comptes rendus physique* (Vol. 15, pp. 761–774). Elsevier Masson SAS. https://doi.org/10.1016/j.crhy.2014.09.010.

Schröder, A., Sprakel, J., Schroën, K., Spaen, J. N., & Berton-Carabin, C. C. (2018). Coalescence stability of pickering emulsions produced with lipid particles: A microfluidic study. *Journal of Food Engineering, 234*, 63–72. https://doi.org/10.1016/j.jfoodeng.2018.04.007

Sommer, A., & Staroszczyk, H. (2023). Bacterial cellulose vs. bacterial cellulose nanocrystals as stabilizer agents for O/W pickering emulsions. *Food Hydrocolloids, 145*. https://doi.org/10.1016/j.foodhyd.2023.109080. Article 109080.

Sun, C., & Gunasekaran, S. (2009). Effects of protein concentration and oil-phase volume fraction on the stability and rheology of menhaden oil-in-water emulsions stabilized by whey protein isolate with xanthan gum. *Food Hydrocolloids, 23*, 165–174. https://doi.org/10.1016/j.foodhyd.2007.12.006

Tang, M. xue, Lei, Y. chen, Wang, Y., Li, D., & Wang, L. jun (2021). Rheological and structural properties of sodium caseinate as influenced by locust bean gum and κ-carrageenan. *Food Hydrocolloids, 112*. https://doi.org/10.1016/j.foodhyd.2020.106251. Article 106251.

Thompson, K. L., Lane, J. A., Derry, M. J., & Armes, S. P. (2015). Non-aqueous isorefractive pickering emulsions. *Langmuir, 31*, 4373–4376. https://doi.org/10.1021/acs.langmuir.5b00630

Varanasi, S., Henzel, L., Mendoza, L., Prathapan, R., Batchelor, W., Tabor, R., & Garnier, G. (2018). Pickering emulsions electrostatically stabilized by cellulose nanocrystals. *Frontiers in Chemistry, 6*. https://doi.org/10.3389/fchem.2018.00409. Article 409.

Vasconcelos, N. F., Feitosa, J. P. A., da Gama, F. M. P., Morais, J. P. S., Andrade, F. K., de Souza Filho, M. de S. M., & Rosa, M. de F. (2017). Bacterial cellulose nanocrystals produced under different hydrolysis conditions: Properties and morphological features. *Carbohydrate Polymers, 155*, 425–431. https://doi.org/10.1016/j.carbpol.2016.08.090

Viennois, E., Bretin, A., Dubé, P. E., Maue, A. C., Dauriat, C. J. G., Barnich, N., Gewirtz, A. T., & Chassaing, B. (2020). Dietary emulsifiers directly impact adherent-invasive E. coli gene expression to drive chronic intestinal inflammation. *Cell Reports, 33*. https://doi.org/10.1016/j.celrep.2020.108229. Article 108229.

Wang, D., Wang, K., Zhao, L., Liu, X., & Hu, Z. (2023). Fabrication and application of pickering emulsion stabilized by high pressure homogenization modified longan shell nanofiber. *Journal of Food Engineering, 339*, Article 111264. https://doi.org/10.1016/j.jfoodeng.2022.111264

Wen, C., Yuan, Q., Liang, H., & Vriesekoop, F. (2014). Preparation and stabilization of d-limonene Pickering emulsions by cellulose nanocrystals. *Carbohydrate Polymers, 112*, 695–700. https://doi.org/10.1016/j.carbpol.2014.06.051

Wong, S. K., Mohd Ali, M. I. A., Low, L. E., Supramaniam, J., Manickam, S., Wong, T. W., Garnier, G., & Tang, S. Y. (2023). Transforming the chemical functionality of nanocellulose for applications in food pickering emulsions: A critical review. In *Food reviews international* (Vol. 40, pp. 1093–1117). Taylor and Francis Ltd. https://doi.org/10.1080/87559129.2023.2212034.

Wu, Y., Lei, C., Li, J., Chen, Y., Liang, H., Li, Y., Li, B., Luo, X., Pei, Y., & Liu, S. (2022). Improvement of O/W emulsion performance by adjusting the interaction between gelatin and bacterial cellulose nanofibrils. *Carbohydrate Polymers, 276*, Article 118806. https://doi.org/10.1016/j.carbpol.2021.118806

Wu, Y., Li, Y., Li, B., Zhang, Y., Wu, Y., & Liu, S. (2023). Effect of surface charge density of bacterial cellulose nanofibrils on the properties of O/W Pickering emulsions co-stabilized with gelatin. *Food Hydrocolloids, 138*. https://doi.org/10.1016/j.foodhyd.2022.108447. Article 108447.

Wu, Y., Zhang, X., Qiu, D., Pei, Y., Li, Y., Li, B., & Liu, S. (2021). Effect of surface charge density of bacterial cellulose nanofibrils on the rheology property of O/W Pickering emulsions. *Food Hydrocolloids, 120*. https://doi.org/10.1016/j.foodhyd.2021.106944. Article 106944.

Xu, Q. Y., Nakajima, M., & Binks, B. P. (2005). Preparation of particle-stabilized oil-in-water emulsions with the microchannel emulsification method. *Colloids and Surfaces A: Physicochemical and Engineering Aspects, 262*, 94–100. https://doi.org/10.1016/j.colsurfa.2005.04.019

Xu, W., Zheng, S., Sun, H., Ning, Y., Jia, Y., Luo, D., Li, Y., & Shah, B. R. (2021). Rheological behavior and microstructure of Pickering emulsions based on different concentrations of gliadin/sodium caseinate nanoparticles. *European Food Research and Technology, 247*, 2621–2633. https://doi.org/10.1007/s00217-021-03827-6

Yan, H., Chen, X., Song, H., Li, J., Feng, Y., Shi, Z., Wang, X., & Lin, Q. (2017). Synthesis of bacterial cellulose and bacterial cellulose nanocrystals for their applications in the stabilization of olive oil pickering emulsion. *Food Hydrocolloids, 72*, 127–135. https://doi.org/10.1016/j.foodhyd.2017.05.044

Zeng, C., Wang, Y., Liu, Y., Su, S., Lu, Y., Qin, S., & Shi, M. (2024). Self-constructed water-in-oil Pickering emulsions as a tool for increasing bioaccessibility of betulin. *Food Chemistry X, 21*. https://doi.org/10.1016/j.fochx.2023.101056. Article 101056.

Zhang, S., Murray, B. S., Holmes, M., Ettelaie, R., & Sarkar, A. (2023). Gastrointestinal fate and fatty acid release of pickering emulsions stabilized by mixtures of plant protein microgels + cellulose particles: An in vitro static digestion study. *Food Biophysics, 18*, 120–132. https://doi.org/10.1007/s11483-022-09756-5

Zhang, H., Qian, Y., Chen, S., & Zhao, Y. (2019). Physicochemical characteristics and emulsification properties of cellulose nanocrystals stabilized O/W pickering emulsions with high -$OSO3^-$ group. *Food Hydrocolloids, 96*, 267–277. https://doi.org/10.1016/j.foodhyd.2019.05.023

Zhang, K., Shen, R., Zhang, Y., Tian, X., & Wang, W. (2024). Modulating in vitro gastrointestinal digestion of nanocellulose-stabilized pickering emulsions by altering particle surface charge. *Food Chemistry, 434*, Article 137521. https://doi.org/10.1016/j.foodchem.2023.137521

Zhang, N., Zang, G. L., Shi, C., Yu, H. Q., & Sheng, G. P. (2016). A novel adsorbent TEMPO-mediated oxidized cellulose nanofibrils modified with PEI: Preparation, characterization, and application for Cu(II) removal. *Journal of Hazardous Materials, 316*, 11–18. https://doi.org/10.1016/j.jhazmat.2016.05.018

Zhao, Y., Khalesi, H., He, J., & Fang, Y. (2023). Application of different hydrocolloids as fat replacer in low-fat dairy products: Ice cream, yogurt and cheese. *Food Hydrocolloids, 138*. https://doi.org/10.1016/j.foodhyd.2023.108493. Article 108493.

Zuppolini, S., Salama, A., Cruz-Maya, I., Guarino, V., & Borriello, A. (2022). Cellulose amphiphilic materials: Chemistry, process and applications. *Pharmaceutics, 14*, 386. https://doi.org/10.3390/pharmaceutics14020386